

Large exchange bias and its connection to interface structure in FeF₂-Fe bilayers

J. Nogués, D. Lederman, T. J. Moran, Ivan K. Schuller, and K. V. Rao

Citation: *Applied Physics Letters* **68**, 3186 (1996); doi: 10.1063/1.115819

View online: <http://dx.doi.org/10.1063/1.115819>

View Table of Contents: <http://scitation.aip.org/content/aip/journal/apl/68/22?ver=pdfcov>

Published by the **AIP Publishing**

Instruments for advanced science

Gas Analysis



- dynamic measurement of reaction gas streams
- catalysis and thermal analysis
- molecular beam studies
- dissolved species probes
- fermentation, environmental and ecological studies

Surface Science



- UHV TPD
- SIMS
- end point detection in ion beam etch
- elemental imaging - surface mapping

Plasma Diagnostics



- plasma source characterization
- etch and deposition process
- reaction kinetic studies
- analysis of neutral and radical species

Vacuum Analysis



- partial pressure measurement and control of process gases
- reactive sputter process control
- vacuum diagnostics
- vacuum coating process monitoring

contact Hiden Analytical for further details

HIDEN
ANALYTICAL

info@hideninc.com
www.HidenAnalytical.com

CLICK to view our product catalogue



Large exchange bias and its connection to interface structure in FeF₂-Fe bilayers

J. Nogués,^{a)} D. Lederman,^{b)} T. J. Moran, and Ivan K. Schuller
Physics Department 0319, University of California-San Diego, La Jolla, California 92093-0319

K. V. Rao
Department of Condensed Matter Physics, Royal Institute of Technology, 10044 Stockholm, Sweden

(Received 8 December 1995; accepted for publication 23 March 1996)

Large exchange bias effects ($\Delta E \sim 1.1$ erg/cm²) were observed in antiferromagnetic (FeF₂)-ferromagnetic (Fe) bilayers grown on MgO. The FeF₂ grows along the spin-compensated (110) direction. The FeF₂-Fe interface roughness was characterized using specular and diffuse x-ray diffraction and atomic force microscopy. The magnitude of the exchange bias field H_E increases as the interface roughness decreases. These results imply that magnetic domain creation in the antiferromagnet plays an important role. © 1996 American Institute of Physics. [S0003-6951(96)02822-7]

Exchange anisotropy (EA), the interfacial interaction between a ferromagnet (FM) and an antiferromagnet (AF), produces a unidirectional interface coupling when a sample is field cooled across the AF Néel temperature. The shift of the FM hysteresis loop away from $H=0$ is known as the exchange bias (H_E). Technological applications include domain stabilizers in magnetoresistive heads and "spin-valve" based devices.^{1,2} Despite extensive work,¹⁻⁵ many questions remain regarding the role of crystalline structure and interface disorder. We have studied the relationship between interface roughness and EA in FeF₂ (AF)-Fe (FM) bilayers. We find a large EA in fully compensated (zero net magnetic moment) FeF₂ surfaces and the highest H_E for the smoothest AF-FM interfaces. These samples have the highest EA energies ever reported for AF-FM bilayer *thin films* ($\Delta E \sim 1.1$ erg/cm²), with a maximum $H_E = 700$ Oe measured in a 6.7 nm thick Fe sample. Models based on domain wall creation in the AF are consistent with our results.

FeF₂ was chosen because of its simple rutile crystal structure, well-known spin structure (inset Fig. 1), and strong uniaxial magnetic anisotropy. Films were grown by sequential *e*-beam evaporations (pressure $< 10^{-6}$ Torr) of FeF₂ (~ 90 nm at a rate of 0.2 nm/s) and Fe (~ 12 nm at a rate of 0.1 nm/s) on MgO (100) substrates. Substrates were heated to 450 °C for 900 s prior to deposition, then cooled to the FeF₂ growth temperature. The Fe layers were always deposited at 150 °C, and capped with ~ 9 nm of Ag to prevent oxidation.

High angle $\Theta - 2\Theta$ *ex situ* x-ray diffraction showed that the FeF₂ grows in the (110) orientation and that the Fe layer is polycrystalline with mainly (110) and (100) orientations. The full width at half-maximum of the (110) rocking curves, $\Delta\Theta = 0.9 - 1.6^\circ$, depends on the growth temperature.

Figure 1 shows the small angle specular x-ray diffraction (SXRD) for samples with the FeF₂ grown at different temperatures. High-frequency peaks correspond to the FeF₂

thickness, while the low frequency envelope corresponds to Fe. Higher FeF₂ deposition temperatures result in lower amplitudes of high frequency peaks, due to an increase in the FeF₂ surface roughness and therefore larger film thickness fluctuations. Quantitative fits using the SUPREX program's⁶ low-angle recursive optical model⁷ adapted for trilayers are shown in Fig. 1. The roughness at the Fe-Ag interface increases with deposition temperature T_S (Table I), although two samples grown at $T_S = 200$ °C have different interface roughness, perhaps due to different substrate roughness. Since the main difference between the samples is the FeF₂ growth temperature, the Fe-Ag interface roughness must be caused by roughness at the FeF₂-Fe interface. We were unable to reproduce the curvature of the (IV) $T_S = 300$ °C sample spectrum with our model.

To determine quantitatively the lateral correlation length

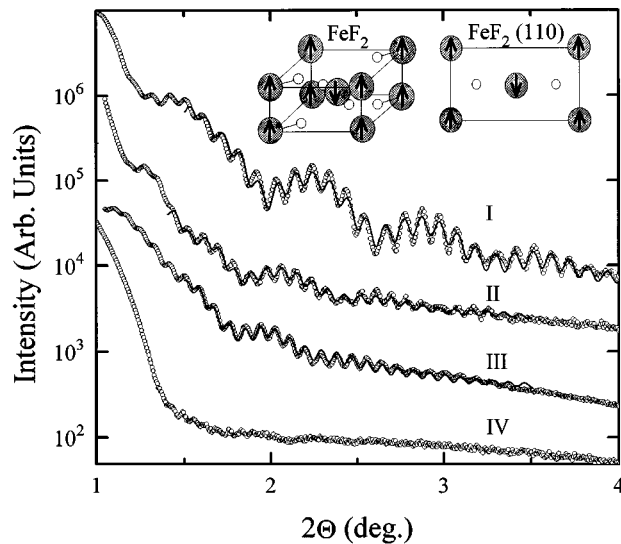


FIG. 1. Small angle x-ray diffraction ($\lambda = 0.15418$ nm) for FeF₂ (~ 90 nm)-Fe (~ 13 nm)-Ag (~ 9 nm) samples with the FeF₂ grown at different temperatures T_S : $T_S = 200$ °C (I), 200 °C (II), 250 °C (III), 300 °C (IV). Solid curves represent fits to optical x-ray model for samples I-III. Samples I and II are from different growth sessions. From top to bottom, fits yielded Fe-Ag interface roughnesses of 0.6, 1.0, and 1.5 nm. Inset: Bulk FeF₂ spin and crystal structure and the corresponding (110) surface spin structure.

^{a)}On leave from the Grup d'Electromagnetisme, Universitat Autònoma de Barcelona, Spain.

^{b)}Present address: Physics Department, West Virginia University, Morgantown, WV 26505-6315.

TABLE I. Fit results of specular x-ray diffraction (SXR), diffuse x-ray diffraction (DXRD), and atomic force microscopy (AFM) data. DXRD and AFM data were obtained in single FeF₂ films. σ is the vertical roughness and ξ the lateral correlation length of σ .

T_S (°C)	σ (nm)			ξ (nm)	
	SXR	DXRD	AFM	DXRD	AFM
200	0.6±0.2	0.10±0.03	1.5±0.1	23±12	58±6
250	1.4±0.2		2.7±0.3		76±8
300		0.18±0.03	3.9±0.4	37±12	91±9

(ξ) of the vertical roughness (σ), single FeF₂ films grown under the same conditions as above were studied by small angle diffuse x-ray diffraction (DXRD) and atomic force microscopy (AFM). Note that these techniques probe the structure at different length scales. DXRD data were analyzed using a model based on the Born approximation.⁸ Variations in χ^2 were not large enough to reliably determine the fractal dimensionality h . However, for fixed values of h , samples grown at higher temperatures had larger average σ and ξ . The results for $T_S = 200$ and 300 °C are shown in Table I and plotted in Fig. 2(a) for $h = 0.5$. σ was calculated from two-dimensional AFM scans by averaging the height fluctuations. ξ was determined by first calculating the two-dimensional height-height autocorrelation function, and then fitting the decay of the correlation function near $R = 0$ to a Gaussian. As in the DXRD results, the AFM σ and ξ increase with T_S [Fig. 2(b) and Table I].

The magnetic characterization was performed using a superconducting quantum interference device magnetometer. Samples were cooled from 120 K through the FeF₂ Néel temperature ($T_N = 78.4$ K), to 10 K in a magnetic field H_{fc} , large enough to saturate the FM layer, parallel to the film surface. The Fig. 3 inset shows hysteresis loops at

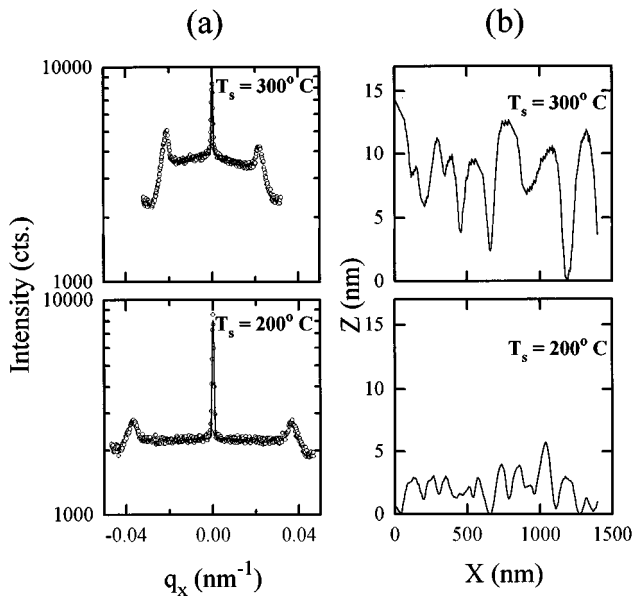


FIG. 2. (a) Diffuse x-ray scattering at $q_z = 1.52$ nm⁻¹ and 1.91 nm⁻¹ for single FeF₂ films grown at $T_S = 300$ °C and 200 °C, respectively. Solid curves represent fits to the model in Ref. 8 with a fixed $h = 0.5$. (b) Atomic force microscopy line scans for single FeF₂ samples grown on MgO at $T_S = 300$ °C and 200 °C.

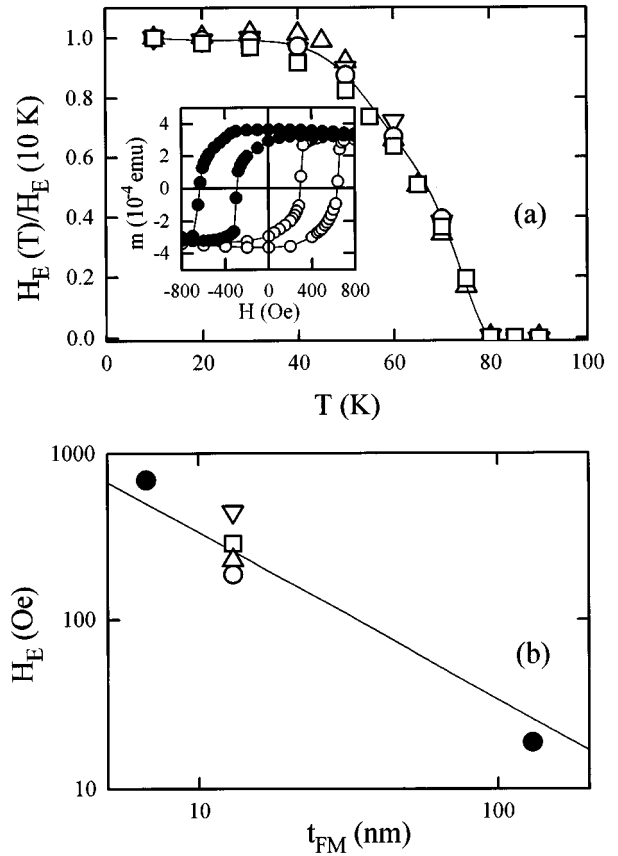


FIG. 3. Exchange bias H_E for samples I (∇), II (\square), III (\triangle), and IV (\circ) in Fig. 1. (a) H_E as a function of temperature normalized to $H_E(10$ K). Inset: Hysteresis loops at $T = 10$ K for FeF₂ (90 nm)–Fe (13 nm)–Ag (9 nm) grown at $T_S = 200$ °C (sample I in Fig. 1) field cooled in 2000 Oe (\bullet) and -2000 Oe (\circ). (b) Log-log plot of $H_E(10$ K) as a function of Fe thickness t_{FM} . (\bullet) are samples grown at $T_S = 200$ °C with thicknesses of 6.7 and 130 nm.

$T = 10$ K for sample (I) cooled in positive and negative fields. Loops were measured in the temperature range $10 < T < 120$ K for $-H_{fc} < H < H_{fc}$. Measuring several consecutive hysteresis loops had no effect on H_E .

The functional form of normalized $H_E(T)$ is insensitive to the interface roughness, as illustrated in Fig. 3(a). However, the low temperature H_E reaches different maxima depending on interface roughness [Fig. 3(b)]. H_E vanishes very close to T_N (i.e., the ‘‘blocking temperature’’ T_B , coincides with T_N), in contrast with other thin film systems^{1,4} where $T_B < T_N$. Together with the above surface analyses, this implies that the low temperature H_E increases as the AF–FM interface becomes smoother.

The magnitude of H_E is usually described in terms of an interface energy per unit area

$$\Delta E = M_{FM} t_{FM} H_E, \quad (1)$$

where M_{FM} and t_{FM} are the magnetization per unit volume and thickness of the ferromagnet respectively. Using the bulk Fe low-temperature saturation magnetization, $M_{FM} = 1740$ Oe, our results are in the range $0.2 < \Delta E < 1.1$ erg/cm².

In the simplest microscopic model, with uncompensated AF surface fixed during the FM magnetization rotation, H_E is a result of the AF–FM interface exchange energy,³

$$\Delta E = \frac{2J_i S^2}{a^2}, \quad (2)$$

where J_i is the exchange at the interface, S is the spin, and a is the lattice parameter. Using the bulk Fe value,⁹ $\Delta E = 17 \text{ erg/cm}^2$, more than one order of magnitude larger than our experimental results. Using the bulk FeF_2 value,¹⁰ $\Delta E = 1.3 \text{ erg/cm}^2$, is much closer to the experimental values.

More sophisticated models rely on the creation of AF domains either perpendicular to the interface, during the field cooling,¹¹ or parallel to the interface, during field reversal.¹²

The first of these models assumes a microscopically random exchange field at the interface, arising from defects, roughness, lattice mismatch, etc. For thick AF films

$$\Delta E = \frac{4zA_{\text{AF}}}{\sqrt{\pi}L}, \quad (3)$$

where z is a factor of order unity, A_{AF} is the AF exchange stiffness and L is the AF domain size. Taking L to be the domain wall size, $L = \pi \sqrt{A_{\text{AF}}/K_{\text{AF}}}$, with K_{AF} being the AF uniaxial anisotropy. Using FeF_2 K_{AF} and J_{AF} values,⁶ $\Delta E = 1.47 \text{ erg/cm}^2$, of the same order of magnitude as our data. This model does not require an uncompensated AF surface, as long as an interfacial random exchange interaction exists which creates small, slightly uncompensated AF domains during cooling. The decrease in H_E could be due to a decrease in random exchange energy resulting from interactions between the FM and less favorable AF crystallographic directions. Moreover, the decrease in H_E could also be due to an increase in L , perhaps due to a lower number of defects in the AF because of the higher growth temperature. Finally, if ξ (Table I) is assumed to correspond to L , then H_E decreases with increasing T_S due to the lateral length scale of the interface disorder.

The second model assumes an AF with anisotropy and an *uncompensated* surface, forcing the creation of AF domain walls parallel to the interface during field reversal. This model predicts an upper limit for the exchange bias, corresponding to spin rotations of 180° away from the AF easy axis,

$$\Delta E = 2\sqrt{A_{\text{AF}}K_{\text{AF}}}. \quad (4)$$

For FeF_2 , $\Delta E = 4.1 \text{ erg/cm}^2$, of the same order of magnitude as our data. The observed H_E decrease with increasing interface roughness would be due to a weakening of the exchange interaction at the interface, thus decreasing the amount of AF spin rotation away from the AF easy axis. This model's ma-

ior deficiency in explaining our data is that it requires an uncompensated surface. However interface reconstruction could result in a net H_E .

Finally, the dependence of H_E on interface roughness seems to contradict recent work on permalloy films grown on CoO (111) single crystals.¹³ This discrepancy may be due to differences in types of disorder, anisotropies, and favorable crystallographic directions.

In conclusion, we have prepared FeF_2 -Fe bilayers, a new system exhibiting a large exchange anisotropy. H_E increases as the interfaces become smoother. This is surprising considering that the bulk FeF_2 spin structure implies a magnetically compensated interface. Models which rely on AF domain creation are in agreement with these results.

We thank S. Sinha and J. M. Gallego for useful discussions, E. E. Fullerton for help with the SUPREX program, and V. Speriosu for motivating our initial interest in exchange anisotropy. This work was supported by the U. S. DOE and NSF. The development of the SUPREX program was supported by the U. S. DOE and the Belgian Interuniversity Attraction Pole Program. J.N. thanks the NATO Scientific Committee and the Spanish Ministerio de Educación y Ciencia for their financial support. After submission of this paper we became aware of large exchange anisotropy in ferrimagnetic-antiferromagnetic bilayers.⁵

¹C. Tsang and R. Fontana, IEEE Trans. Magn. **18**, 1149 (1982).

²B. Dieny, J. Magn. Mater. **136**, 335 (1994).

³W. H. Meiklejohn and C. P. Bean, Phys. Rev. **105**, 904 (1957).

⁴W. C. Cain and M. H. Kryder, J. Appl. Phys. **67**, 5722 (1990); M. J. Carey and A. E. Berkowitz, Appl. Phys. Lett. **60**, 3060 (1992); R. Jungbult, R. Coehoorn, M. T. Johnson, C. Sauer, P. J. van der Zaag, A. R. Ball, T. G. S. M. Rijks, J. aan de Stegge, and A. Reinders, J. Magn. Mater. **148**, 300 (1995).

⁵P. J. van der Zaag, R. M. Wolk, A. R. Ball, C. Bordel, L. F. Feiner, and R. Jungbult, J. Magn. Mater. **148**, 346 (1995).

⁶I. K. Schuller, Phys. Rev. Lett. **44**, 1597 (1980); W. Sevenhans, M. Gijs, Y. Bruynseraede, H. Homma, and I. K. Schuller, Phys. Rev. B **34**, 5955 (1986); E. E. Fullerton, I. K. Schuller, H. Vanderstraeten, and Y. Bruynseraede, *ibid.* **45**, 9292 (1992).

⁷B. Vidal and P. Vincent, Appl. Opt. **23**, 1794 (1984).

⁸S. K. Sinha, E. B. Sirota, G. Garoff, and H. B. Stanley, Phys. Rev. B **38**, 2297 (1988).

⁹C. Kittel, *Introduction to Solid State Physics*, 6th ed. (Wiley, New York, 1986), p. 424.

¹⁰M. T. Hutchings, B. D. Rainford, and H. J. Guggenheim, J. Phys. C **3**, 307 (1970).

¹¹A. P. Malozemoff, Phys. Rev. B **37**, 7673 (1988).

¹²D. Mauri, H. C. Siegmann, P. S. Bagus, and E. Kay, J. Appl. Phys. **62**, 3047 (1987).

¹³T. J. Moran, J. M. Gallego, and I. K. Schuller, J. Appl. Phys. **78**, 1887 (1995).